Thermal Conductivity of Heavily Doped p-Type InSb at Liquid-Helium Temperatures*

C. R. Crosby and C. G. Grenier
Department of Physics and Astronomy, Louisiana State University, Baton Rouge, Louisiana 70803
(Received 22 March 1971)

The lattice thermal conductivity λ_g of three heavily doped ($>10^{18}$ cm^{-3}) p-type samples of InSb has been determined in the temperature range 1.3–4.2 °K. The data are fitted to a phenomenological model including boundary scattering, Rayleigh scattering due to impurities and isotopes, and the scattering of phonons by charge carriers. That the charge carriers are a significant source of scattering is indicated by a general T^2 behavior at the lowest temperatures and by a rapid increase in λ_g at the higher temperatures because of phonons which have wave-propagation vectors larger than the diameter of the Fermi surface, and which therefore cannot be scattered by charge carriers. A probable screening in the carrier-phonon interaction is apparent from the lowest-temperature behavior of λ_g. In general, a good fit is made using the theories of charge-carrier–phonon interactions developed for the treatment of ultrasonic attenuation.

I. INTRODUCTION

This work covers measurement and analysis of the thermal conductivity in heavily doped degenerate p-type InSb in the liquid-helium temperature range. Earlier work on p-InSb by Challis *et al.*[1] indicated that a quantitative study of the electron-phonon scattering could be obtained should higher doping concentrations be used. The relatively simple way in which the hole distribution is affected by doping was expected to yield more straightforward analysis than in the case of Sb studied in a previous work.[2]

The principal features of the thermal conductivity which in this work would strongly confirm phonon scattering by charge carriers are (a) a general tendency toward a T^2 dependence in the proper temperature range, (b) a rapid increase at the high-temperature range similar to the effect of the cutoff in the phonon-electron interaction for phonons with wave-propagation vector larger than the diameter $2k_F$ of the Fermi surface (FS) (the variation of $2k_F$ with the doping concentration allows some detailed study of this point), (c) a departure from the T^2 dependence of the thermal conductivity at the lowest temperatures which would empirically agree with the screening[3] of the phonon-electron interaction in the regime of the long-wavelength phonons, and (d) a good fit with the relevant theories.

Theory[3–10] developed for the electron-phonon interaction in ultrasonic attenuation seems to adapt well for this case, and also probably could explain some similar anomalies found in other heavily doped semiconductors.[11–13]

Section II is a brief description of the experimental procedure. Section III presents the development of the theoretical expressions to which the data are compared. Section IV consists of the results and discussion of the thermal-conductivity measurement. Section V presents the conclusions drawn from this study.

II. EXPERIMENTAL DETAILS

The samples were obtained from Cominco American.[14] They were rectangular parallelepipeds cut from heavily doped p-type single-crystal InSb to have cross-section dimensions 2×4 mm, and to be as long as possible with the [111] axis perpendicular to within 5° of the large face. Sample A was 22 mm long and doped with zinc. Samples B and C were cadmium doped with lengths of 30 and 28 mm, respectively. The surfaces of the crystals as received were lapped.

The measurement of the thermal resistivity was made using a steady-state heat-flow method. Two Allen-Bradley carbon-resistor thermometers (51Ω, $\frac{1}{8}$ W) were used to measure the temperature at two points along the InSb samples. The thermometers were constructed by wrapping the resistors tightly with 38-gauge Formvar-coated copper wire, the ends of which were brought together, twisted, and soldered to the sample. The sample heater consisted of 44-gauge Constantan wire wound on a horseshoe-shaped piece of 20-gauge copper wire which was soldered to one end of the crystal. The other end of the sample was soldered to a copper piece which was firmly clamped to the heat sink which extended outside the evacuated container in which the sample crystal, thermometers, and heater were placed. This container was submerged in the liquid-helium bath. All soldering was done with pure indium. Electrical leads from the heater to the helium bath were superconducting niobium.

Characteristic data on the samples used are given in Table I. The quantities n, l, and ϵ_F, cor-

responding, respectively, to the carrier density, mean free path, and chemical potential, were obtained from Hall-effect and resistivity measurements at liquid-helium temperatures under the simplifying assumption of a single isotropic quadratic band. The expression used to determine the density of carriers is valid for a single band or in the high-magnetic-field limit for a material with multiple bands. The measurements of ρ_{21} were made up to 6 kOe, which (considering the doping levels) is a low-field regime for p-type InSb. The error induced by using the low-field values of ρ_{21} in the high-field expression for the carrier density may be as high as 50%.[15]

III. THEORY

The analysis of the experimental results uses an expression for the lattice conductivity[16] in the limit of weak-phonon mixing. This expression, assuming isotropy and nondispersion in the phonon spectrum, is

$$\lambda_g = \frac{K}{2\pi^2 s}\left(\frac{KT}{\hbar}\right)^3 \int_0^{\Theta/T} \tau \frac{x^4 e^x}{(e^x-1)^2}\, dx , \qquad (1)$$

where no distinction between transverse and longitudinal phonon modes is made. In Eq. (1), s is an averaged value of the velocity of sound, $x = \hbar s q/KT$, where q is the magnitude of the phonon wave vector, τ is a q-dependent relaxation time, and Θ is the Debye temperature. At low temperatures where Θ/T is large (Θ for InSb is approximately 200 °K[17]) the upper limit of the integral will be taken as infinite with negligible error.

When a distinction between longitudinal and transverse sound waves is to be made under the same condtions as above, the conductivity is of the form

$$\lambda_g = \frac{K}{6\pi^2}\left(\frac{KT}{\hbar}\right)^3 \int_0^{\infty} \left(\frac{\tau_L}{s_L} + \frac{2\tau_T}{s_T}\right) \frac{x^4 e^x}{(e^x-1)^2}\, dx , \qquad (2)$$

where the indices L and T refer to longitudinal and transverse modes, respectively. In either case, the phonon relaxation time τ is obtained assuming the principle of additivity of scattering frequencies as

$$\tau^{-1} = \tau_b^{-1} + \tau_c^{-1} + \tau_i^{-1} , \qquad (3)$$

where the scattering due to boundaries, charge carriers, and impurities, respectively, are included and all other mechanisms are neglected.

A. Boundary Scattering

The scattering-relaxation frequency arising from crystal boundaries is given by the ratio of the velocity of sound to the Casimir[18] length L and is a constant:

$$\tau_b^{-1} = B = s/L . \qquad (4)$$

The Casimir length for a sample of rectangular cross section of area S is such that $\frac{1}{4}\pi L^2 = S$.

B. Impurity Scattering

The impurity-scattering frequency τ_i^{-1} is somewhat complex and can be decomposed as the sum of terms

$$\tau_i^{-1} = \tau_{iso}^{-1} + \tau_{im}^{-1} + \tau_{is}^{-1} + \tau_{ir}^{-1} + \tau_k^{-1} . \qquad (5)$$

The first three terms are Rayleigh-type scattering, i.e., proportional to the fourth power of the phonon wave vector,

$$\tau_i^{-1} = Dq^4 = dx^4 T^4 , \qquad (6)$$

where D is the constant of proportionality and $d = D(K/\hbar s)^4$. More specifically, τ_{iso}^{-1} and τ_{im}^{-1} are the mass-difference scattering due to isotope and impurities substitution, and the combined D value for mass-difference scattering is given by

$$D_m = (s/4\pi N^2)\textstyle\sum_j N_j (1 - M_j/\bar{M})^2 .$$

Here the molecule is InSb and the summation is carried over all the kinds of molecules AB formed by the different isotope and impurity atoms. N_j and M_j correspond, respectively, to the number per unit volume and the mass of a given kind of molecule (AB), $\bar{M}$ is the average molecular mass, and N is the number of AB molecules per unit volume.

The other Rayleigh-scattering term τ_{is}^{-1} is a strain scattering caused by force-constant difference and volume difference[19] associated with the impurities. We have

$$\tau_{is}^{-1} = \frac{s}{2\pi N^2}\sum_j N_j \left(\frac{\Delta F}{F} - \frac{4\Delta V}{V}\right)_j^2 = D_s q^4 ,$$

TABLE I. Quantities determined from Hall-effect and resistivity measurements. $n = H/ec\rho_{21}$, $\tau_e = m\sigma_0/ne^2$, $k_F = (3\pi^2 n)^{1/3}$, $l = \hbar k_F \tau_e/m$, and $\epsilon_F = \hbar^2 k_F^2/2m$ where ρ_{21} is the Hall resistivity, σ_0 is the dc conductivity, and $m = 0.4m_0$ is the heavy-hole effective mass.

Sample	n (10^{18} cm^{-3})	σ_0 (Ω^{-1} cm^{-1})	τ_e (10^{-13} sec)	$2k_F$ (10^7 cm^{-1})	l (10^{-6} cm)	ϵ_F (meV)
A	1.08	136.0	1.8	1.01	1.65	24.0
B	2.20	218.0	1.4	1.16	1.64	32.0
C	7.60	537.0	1.0	1.51	1.77	54.0

where N_j is the number of j-type impurities and $\Delta F/F$ and $\Delta V/V$ are, respectively, the added stress and added dilatation introduced by the impurity. The addition of D_s, for which there is not sufficient information to calculate, may account for part of the discrepancy between the experimentally determined value D and the calculated value for D_m.

A resonance-scattering term τ_{ir}^{-1} of the type formulated by Pohl,[20]

$$\tau_{ir}^{-1} \propto \frac{\omega^2 T^n}{(\omega_0^2-\omega^2)^2+(\Omega/\pi)^2\omega^2\omega_0^2} , \tag{7}$$

may modify the simple Rayleigh-type behavior, but its effect is generally expected in a temperature range higher than the range reported here, and therefore will not be considered. Here ω_0 is the resonance frequency and Ω describes damping of the resonance.

The last impurity-scattering term of Eq. (5) is due to resonancelike bound electron-phonon processes of the type proposed by Keyes[11,21]:

$$\tau_k^{-1} \propto \omega^4[\omega^2-(4\Delta/\hbar)^2]^{-2}[1+r_0^2\omega^2/4s^2]^{-8} , \tag{8}$$

where 4Δ is the chemical shift related to the splitting of electronic states, and r_0 is the mean radius of the localized state. If in p-InSb it is assumed that $\hbar\omega < 4\Delta$, then the resonance term vanishes. The scattering appears then to be of the Rayleigh type with a cutoff for $q > 4/r_0$, where r_0 is the orbit radius of the electron or hole in the hydrogenlike state of the impurity. One may expect this cutoff to be concentration independent, and to be well defined only for low concentrations of impurities.

In summary, the impurity-scattering frequency τ_i^{-1} can be approximated by a Rayleigh term $\tau_i^{-1} = Dq^4$. The deviation from this simple behavior due to τ_{ir}^{-1} and τ_k^{-1} will be neglected with some justification given in Sec. IV. With this simplification, one notes that both the coefficient B of the size scattering and D of the impurity scattering are proportional to s. Should distinction be made between longitudinal and transverse phonons, the corresponding B and D terms will be expected to be proportional to their corresponding velocities.

C. Charge-Carrier–Phonon Scattering in Semiconductors

Considering the electron-phonon scattering due to charge carriers, Ziman[22] derived the relaxation time for the case in which the carriers are contained in a parabolic isotropic band and the density of the carriers is large enough that $T_F > T$, where the temperature T_F is defined by $KT_F = \hbar^2 k_F^2/2m$. Ziman showed that the scattering frequency is of the form

$$\tau_c^{-1} = \Omega_c(q) F_z(q) , \tag{9}$$

where $F_z(q)$ is a cutoff function which takes account of the fact that not every phonon can be scattered. This can be understood by the simple consideration of momentum conservation. When the electron is scattered from a state characterized by a vector $\vec{k}$ to a state characterized by $\vec{k}'$, with $\vec{k}' = \vec{q} + \vec{k}$, the limit $q \leq 2k_F$ is set on $\vec{q}$ owing to the upper limit k_F taken by both $\vec{k}$ and $\vec{k}'$. One may expect a cutoff function $F(q) = 1$ for $q \leq 2k_F$ and $F(q) = 0$ for $q > 2k_F$. This is what in practice is realized by Ziman's cutoff function $F_z(q)$. Taking into consideration both momentum and energy conservation, $F_z(q)$ is determined to be

$$F_z(q) = 1 - \frac{kT}{\hbar q s} \times \ln \frac{1+\exp\{(kT)^{-1}[\frac{1}{2}\hbar q s - (\hbar^2/8m)(4k_F^2 - q^2)]\}}{1+\exp\{(kT)^{-1}[-\frac{1}{2}\hbar q s - (\hbar^2/8m)(4k_f^2 - q^2)]\}}$$

or

$$F_z(q) = \frac{1}{x} \ln \frac{e^{x/2}+\exp\{-(T/16T_s)[(\Theta^*/T)^2 - x^2]\}}{e^{-x/2}+\exp\{-(T/16T_s)[(\Theta^*/T)^2 - x^2]\}} , \tag{10}$$

where m is the effective mass of the carrier and

$$\Theta^* = 2k_F(\hbar s/K) = (4T_F T_s)^{1/2} \tag{11}$$

is a parameter of interest to characterize low-temperature transport effects.[2,23] The temperature T_s is defined by $KT_s = \frac{1}{2}ms^2$.

The scattering function $\Omega_c(q)$ is taken by Ziman to have the simple form

$$\Omega_c(q) = Aq = axT , \tag{12}$$

with $A = m^2C^2/2\pi\rho\hbar^3$ and $a = Km^2C^2/2\pi\rho s\hbar^4$, where C is the deformation potential and ρ is the mass density. It is generally argued that the local strain induced by the sound wave changes the energy of the charge carriers by the amount

$$\delta E(\vec{r}) = \sum_{ij} C_{ij}\Delta_{ij}(\vec{r}) ,$$

where the C_{ij} are the components of the deformation-potential tensor and the $\Delta_{ij}(\vec{r})$ are the components of the local strain.

When an analysis of the conductivity is made using Eqs. (1), (3), (4), (6), (9), (10), and (12) with proper adjustment of parameters, a relatively good fit is obtained at the highest temperatures concurring with the evidence of the Ziman cutoff of the carrier scattering. However, at the low-temperature end there are indications that the simple linear term $\Omega(q) = Aq$ overestimates the scattering of the low-q phonons. This is to be expected from qualitative considerations. When the phonon wavelength becomes of the order of or larger than the carrier mean free path, i.e., $ql \lesssim 1$, a decrease in the strength of the interaction should occur. Also, the electron system reacts as a plasma to low-frequency phonons, and the resulting screen-

ing decreases the phonon-electron interaction. A number of theories[3-10] have been worked out in the field of acoustic attenuation which bring about these features. For reasons of unity, the treatment by Cohen *et al.*[3] with the extension of Harrison[4] and Spector[5] (CHS) is used here with some slight modifications. Referring to Eq. (2.13) given by Spector,[5] one has

$$\Omega(q)=\frac{nm_0^2}{\tau_e\rho m}\,\mathrm{Re}\,\vec{\mu}\cdot\left(\frac{m}{m_0}+\overleftrightarrow{B}-\frac{\tau_e\overleftrightarrow{C}\cdot\vec{q}\vec{q}\cdot\overleftrightarrow{B}}{im_0\omega}\right)\times(\overleftrightarrow{\sigma}'+\overleftrightarrow{B})^{-1}\left(\frac{m}{m_0}-\overleftrightarrow{\sigma}'+\frac{\tau_e\overleftrightarrow{\sigma}'\cdot\vec{q}\vec{q}\cdot\overleftrightarrow{C}}{im_0\omega}\right)\cdot\vec{\mu}^{*}\,. \tag{13}$$

If the 1 direction is chosen to be in the direction of q, then $\overleftrightarrow{B}$ is a diagonal tensor with $B_{11}=-i\gamma$, $B_{22}=B_{33}=i\gamma c^2/s^2$, where c is the velocity of light, $\overleftrightarrow{C}$ is the symmetrical deformation-potential tensor, $\vec{\mu}$ is a unit polarization vector, $\overleftrightarrow{\sigma}'$ is the diagonal reduced-conductivity tensor

$$\overleftrightarrow{\sigma}'=(\overleftrightarrow{\sigma}/\sigma_0)(1-\alpha\overleftrightarrow{R})^{-1}\,, \tag{14}$$

$\overleftrightarrow{R}$ is a tensor with all components zero except $R_{11}=p/i\omega\tau_e$ and $\overleftrightarrow{\sigma}$ is the diagonal conductivity tensor with relevant components

$$\sigma_{11}=3\sigma_0\frac{1-i\omega\tau_e}{(ql)^2}p,\qquad \sigma_{22}=\sigma_{33}=\frac{3\sigma_0}{2}\left(\frac{1-p}{1-i\omega\tau_e}-\frac{(1-i\omega\tau_e)}{(ql)^2}p\right), \tag{15}$$

where

$$p=1-\tfrac{1}{2}\int_{-1}^{1}[1-iyql(1-i\omega\tau_e)^{-1}]^{-1}\,dy\,. \tag{16}$$

Other terms introduced here are τ_e, the carrier relaxation time, l, the carrier mean free path, ω, the phonon frequency, $\gamma=\omega/\omega_p^2\tau_e$, where $\omega_p=(4\pi\sigma_0/\tau_e\epsilon)^{1/2}$, and ϵ, the static dielectric constant. In Eq. (13) a distinction is being made between m_0 and m—the free and effective masses of the carriers—to take account of Harrison's remark[4] that the drag and energy feedback involve the free mass of the carrier. A coefficient α has been introduced in $\overleftrightarrow{\sigma}'$ to take account of the possibility of recombination, ionization, or carrier trapping.[24]

The resulting scattering frequency for longitudinal and transverse phonons becomes, respectively,

$$\Omega_L(q)=\frac{nm_0^2}{\tau_e\rho m}\,\mathrm{Re}\left[\left(\frac{m}{m_0}+B_{11}-\frac{\tau_e q^2B_{11}C_{11}}{i\omega m_0}\right)\times\left(\frac{m}{m_0}-\sigma_{11}'+\frac{\sigma_{11}\tau_e q^2C_{11}}{i\omega m_0}\right)\Big/(\sigma_{11}+B_{11})\right], \tag{17a}$$

$$\Omega_T(q)=\frac{nm_0^2}{\tau_e\rho m}\,\mathrm{Re}\left(\frac{(m/m_0-\sigma_{22}')(m/m_0+B_{22})}{\sigma_{22}'+B_{22}}+\frac{B_{11}\sigma_{11}'q^4\tau_e^2C_{12}^{\,2}}{(\sigma_{11}'+B_{11})m_0^2\omega^2}\right). \tag{17b}$$

These equations were used at first in the scattering computation, but it was found that to within 1%, only the deformation-potential terms were significant, and that for present purposes Eqs. (17) were approximated by

$$\Omega_L(q)=\frac{n\tau_e}{\rho}q^2\frac{C_{11}^{\,2}}{ms_L^2}\Sigma(q,s_L)\,,\qquad \Omega_T(q)=\frac{n\tau_e}{\rho}q^2\frac{C_{12}^{\,2}}{ms_T^2}\Sigma(q,s_T)\,, \tag{18}$$

where

$$\Sigma=\mathrm{Re}\left(\frac{\sigma_{11}'B_{11}}{\sigma_{11}'+B_{11}}\right) \tag{19}$$

is the reduced conductance of the two impedances $1/\sigma_{11}'$ and $1/B_{11}$ in series.

It is interesting to note that the scattering terms in Eq. (18) exhibit the same q dependency, as opposed to the case of metals where the scattering frequencies for the different phonon polarizations appear as completely different functions of the phonon wave vector. In the range of interest here one finds $\Sigma_L/\Sigma_T\simeq(s_L/s_T)^2$ and thus $\Omega_L(q)/\Omega_T(q)\simeq(C_{11}/C_{12})^2$. This is an indication that the simplified analysis based on Eq. (1), as compared to the analysis through Eq. (2), will correspond to a relevant approximation, and that the empirically determined scattering in this simplified analysis will be representative of the basic scattering involved in the InSb samples studied. More specifically, when

$$l_e^{-1}<q_{TF}<q<2k_F\,, \tag{20}$$

the value Σ simplifies and Eq. (18) yields the term used in Ziman's theory for $\Omega(q)$, i.e., Eq. (12). In (20) $q_{TF}=\omega_p/v_F$ is the Thomas-Fermi wave vector and v_F is the Fermi velocity of the carriers.

If the phonon–charge-carrier scattering is preponderant over τ_b^{-1} and τ_i^{-1}, and if one considers the temperature range where contribution to the heat conduction comes mostly from phonons satisfying condition (20), it is expected that the lattice thermal conductivity λ_g will exhibit the usual T^2 law

$$\lambda_g=(7.212\hbar K^3\rho/\pi m^2)C^{-2}T^2\,,$$

or

$$\lambda_g=(7.212\hbar K^3\rho/\pi m^2)(\tfrac{1}{3}C_{11}^{-2}+\tfrac{2}{3}C_{12}^{-2})T^2\,, \tag{21}$$

using Eqs. (1) and (2), respectively. Therefore, it may be seen that the average over modes yields for the averaged deformation potential the relation

$$C^{-2}=\tfrac{1}{3}C_{11}^{-2}+\tfrac{2}{3}C_{12}^{-2}\,. \tag{22}$$

The components of the deformation potential in fact depend on the direction in which $\tilde{q}$ is taken in the crystal. However, the calculation of λ_g involves an averaging over all $\tilde{q}$ directions so that the C_{11} and C_{12} appearing in Eq. (22) may be considered as averaged quantities.

Outside of the $\lambda_g \propto T^2$ range the averaging over the different scattering is less clear. At the higher temperatures where phonons with $q \approx 2k_F$ have to be considered, Ziman's cutoff $F_g(q)$, as expressed as a function of x in Eq. (2), occurs for the different values of x, Θ_L^*/T and Θ_T^*/T, for the different polarizations. Therefore, in the simplified analysis where a single cutoff is used instead of two, some indetermination will result mainly in the averaged impurity-scattering term. The impurity scattering is indeed the principal scattering once the carrier scattering is cut off. It is questionable whether or not the refinement made by inclusion of the double cutoff might be offset by the ambiguity in the determination of the Θ^* [Eq. (11)] due to anisotropy in the phonon and electron distributions.

At lower temperatures where phonons with $q \approx q_{TF}$ have to be considered, the Σ function takes a complicated form which nevertheless simplifies if $ql \gg 1$ for which the scattering becomes

$$\Omega(q) = Aq[1 + 3(q_{TF}/q)^2]^{-2}, \qquad (23)$$

which is a conveniently simple formulation of the plasma screening cutoff. Thus for $q > q_{TF}$ the scattering approaches the unscreened term given by Eq. (12), whereas for $q < q_{TF}$ the screening effect for small q makes the carrier scattering term fall sharply.

IV. RESULTS AND DISCUSSION

In the analysis of the conductivity it was felt that the simple form of Eq. (1), where phonon polarization is not distinguished, could be used to determine the nature of scattering, subject to the restrictions discussed above. An averaged value for the velocity of sound $s = 2.26 \times 10^5$ cm/sec[17] is used in the different computations, except when specific distinction between polarizations is made in the discussion, in which cases s_L and s_T averages are taken as $s_L = 3.77 \times 10^5$ cm/sec and $s_T = 1.88 \times 10^5$ cm/sec. The values for n,[15] τ_e, and l are taken from Table I. The hole mass used is $m = 0.4\ m_0$[25] and the static dielectric constant $\epsilon = 18$.[25] From those basic quantities, one can derive such quantities as k_F, Θ^*, Θ_L^*, Θ_T^*, v_F, ω_p, and q_{TF} for the different samples as well as D_m if one supposes the impurity density is given by $N_i = n$. In principle, only C is an unknown quantity to be determined. But it was found that a better fit between theory and experiment was achieved when other quantities such as Θ^*, d, and q_{TF} were treated as parameters and adjusted to fit the experiment. Then comparison between experimental and computed values for these parameters would serve as a check into the theory and the validities of the approximations.

The values of C, d, Θ^*, and q_{TF} obtained for a best fit are presented in Table II along with calculated values of d_m, Θ^*, and q_{TF} for each sample. The results of the calculation of λ_g using the values in Table II are represented by the solid curves which accompany the experimental data points in Fig. 1.

The curves fitted to the experimental data are quite sensitive to the deformation potential since it is the principal parameter which determines the depth of the minimum for the λ_g/T^2-vs-T curve. The values of the deformation potential obtained are within the range expected.[11,26] There seems to be a slight dependency of the deformation potential on the impurity concentration, with the magnitude of C decreasing as n increases.

The effective Debye temperatures Θ^* resulting from the analysis are in the same sequence, but are larger than the values calculated from the measured carrier densities. As mentioned earlier, the Θ^* for each sample should probably not be a single value but take on a range of values between Θ_T^* and Θ_L^*. The Θ^* obtained experimentally for all three samples are in the range between the calculated values for Θ_T^* and Θ_L^*, and should the correction implied in Ref. 15 be performed a still better match would be obtained. The analysis is reasonably sensitive to Θ^* as this parameter located the minimum along the temperature axis and in conjunction with the parameter d determined the slope above the minimum.

The introduction of the Thomas-Fermi wave

TABLE II. Parameters determined from analysis of data using Eq. (1) along with calculated values of d_m, Θ^*, and q_{TF}. Here q_{TF}^e is the value arising from the curve fit and q_{TF}^c is the theoretical value of the Thomas-Fermi wave vector calculated from the relation $q_{TF} = \omega_p/v_F$, where ω_p is the plasma frequency and v_F is the Fermi velocity.

Sample	C (eV)	d ($^\circ$K^{-4} sec^{-1})	d_m ($^\circ$K^{-4} sec^{-1})	Θ^* ($^\circ$K)	Θ_{CALC}^* ($^\circ$K)	q_{TF}^e (10^6 cm^{-1})	q_{TF}^c (10^6 cm^{-1})
A	-1.18	13.5	3.2	17.5	11.0	0.82	2.38
B	-1.12	20.0	2.8	20.0	14.0	0.80	2.68
C	-1.06	25.0	2.9	26.0	21.1	0.75	3.29

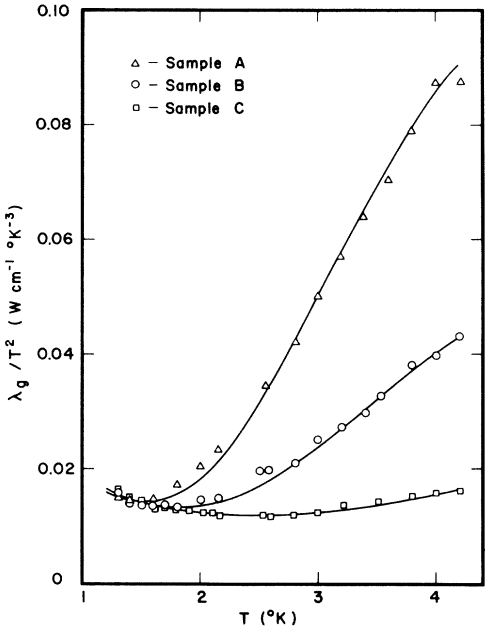

FIG. 1. Lattice thermal conductivity λ_g of three samples of heavily doped p-type InSb, multiplied by T^{-2} vs T in a linear plot. The way in which the individual sets of data break away from the low-temperature nearly T^2 dependence of λ_g is indicative of the abrupt cutoff in scattering by charge carriers of phonons with $q > 2k_F$. The sequence in which these cutoffs occur follows the sequence of increase of $2k_F$ due to increased doping. The somewhat-less-than-T^2 behavior at the lowest temperatures is attributed to screening of the charge-carrier–phonon interaction for low-q phonons. The solid curves are computed from Eq. (1) using parameters listed in Tables I and II.

vector as a parameter allows control of the amount of screening by delaying the onset of screening as q_{TF} is decreased. That some control over screening is necessary is indicated in Fig. 2, where the data for sample B are presented, along with solid curves representing best fits using the carrier scattering represented by Eq. (12), where there is no screening (curve 1), CHS with the full effect of screening (curve 2), and CHS with the screening reduced by adjustment of q_{TF} (curve 3). Table II shows that the values of q_{TF} obtained by curve fitting are much smaller than those calculated, varying from 34% of the expected value for sample A to only 23% for sample C. By comparison Challis No. 6 sample with less doping yields 42%. It may be noted that the purer the sample the closer to the theoretical expectation for q_{TF}. Attempts to explain such a small empirical value of the parameter used in place of the Thomas-Fermi wave vector will be made later.

To illustrate the different types of phonon scattering as obtained for sample B, the phonon-scattering frequencies due to the three principal scattering mechanisms are shown in dashed lines in Fig. 3 as functions of the phonon wave vector with the sum of the scattering frequencies as the solid curve. In Fig. 3 the carrier scattering displays the very rapid fall due to screening when the phonon wave vector is of the order of q^e_{TF} or less. Other features apparent in Fig. 3 are the very abrupt cutoff of charge-carrier scattering at $2k_F$ as calculated for $T = 2\,^\circ$K and the linear wave-vector dependence of the carrier-scattering frequency for $q > q_{TF}$ which agree with the Ziman theory. The boundary scattering appears as the term independent of q.

It can easily be seen that an increase in the scattering due to crystal boundaries would compensate in part the effect of screening in the low-q region. However, to fit the experimental behavior of λ_g in this region by adjusting τ_b^{-1} would require an unjustifiable order-of-magnitude increase in boundary scattering.

A number of other possible explanations for the discrepancy between experimental and theoretical values of q_{TF} or for partial compensation of the screening effect have been examined. The case of additional bands of scatterers lends itself to a relatively simple study which is given here in some detail.

Awareness of the fact that semimetals such as

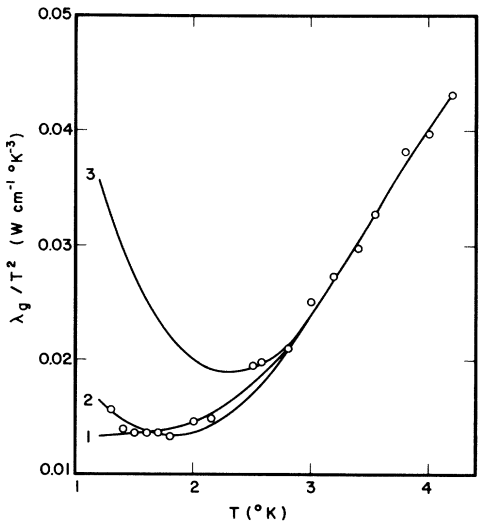

FIG. 2. Lattice thermal conductivity of sample B, multiplied by T^{-2} vs T in a linear plot, showing the effects of screening of the charge-carrier–phonon interaction for low-q phonons. Curve 3 uses Eq. (1) with parameters listed in Tables I and II with the value of q^c_{TF} which introduces the full theoretical effects of screening. Curve 2 was computed exactly as curve 3 with the exception that q_{TF} was adjusted to the value of q^e_{TF} to reduce the screening. Curve 1 is a fit to the data with no screening. The parameters for this curve were adjusted to give a best fit and are somewhat different than those for curves 2 and 3.

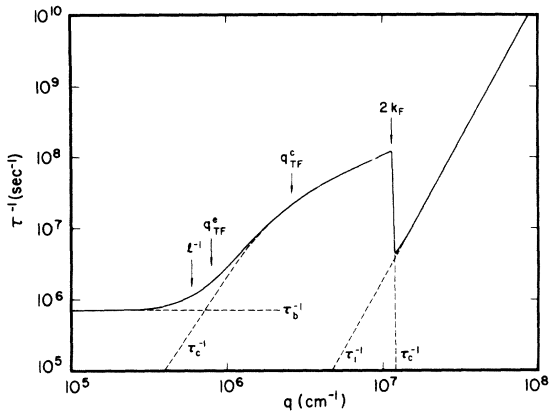

FIG. 3. Sum τ^{-1} of the separate scattering frequencies, τ_b^{-1}, τ_c^{-1}, and τ_i^{-1} vs the magnitude of the phonon wave vector q in a log-log plot for sample B at 2 °K with $q_{TF} = q^e_{TF}$. Principal features of this plot are the cutoff in charge-carrier scattering τ_c^{-1} at $2k_F$, the linear-in-q dependence of τ_c^{-1} just below $2k_F$, and the rapid decrease in τ_c^{-1} below q^e_{TF}. Also indicated are the q^4-dependent impurity scattering τ_i^{-1} for high-q phonons and the q-independent boundary scattering τ_b^{-1}, which comes into prominence at the low end of the phonon spectrum.

antimony, which have many similarities to degenerate semiconductors, show only a limited amount of screening was a clue in the search for a reason for the unexpectedly small empirical values of q_{TF}. Usually in semimetals, carrier compensation is cited as the cause for the absence of screening, even though a less restrictive condition such as the existence of multiple bands without compensation would be sufficient to diminish the screening. In this respect, there are two possibilities for an additional band in the samples under study: first, an impurity band[27] and second, the light-hole band which is degenerate with the principal heavy-hole band at the center of the zone. Eckstein[10] has developed the theory of charge-carrier–phonon interactions for the case where there are two compensated bands of carriers. From this theory, the expression for the relaxation frequency can be established in a relatively simplified form when only deformation-potential scattering terms are considered. The resulting expression, which is valid even if there is no compensation, is

$$\Omega(q) = \frac{q^2}{\rho e^2 s^2} \operatorname{Re}\left(\frac{\sigma_1\sigma_2(C_1 \pm C_2)^2 + B'(\sigma_1 C_1^2 + \sigma_2 C_2^2)}{\sigma_1 + \sigma_2 + B'}\right), \tag{24}$$

where the + sign is used when the sign of the carriers of bands 1 and 2 are different. Here $B' = ie\omega/4\pi$ and $\sigma_i = \sigma_i^0 \sigma_{i11}'$, where the σ_i^0 are the dc conductivities with $\sigma_2^0 < \sigma_1^0 \approx \sigma_0$, σ_{i11}' is the 11 component of σ' for the ith band, and the C_i are either the 11 or 12 components of the deformation-potential tensor, depending on whether the relaxation frequency for longitudinal or transverse waves is desired. One may note that for $\sigma_2 = 0$, Eq. (24) reduces to Eq. (17), the limiting form obtained by CHS for a single band.

In the case where $|B'| \gg |\sigma_1|$, which is roughly equivalent to $q > q_{TF}$, this becomes

$$\Omega(q) = (q^2/\rho e^2 s^2)\operatorname{Re}(\sigma_1 C_1^2 + \sigma_2 C_2^2)\,. \tag{25}$$

However, for small q where $|B'| \ll |\sigma_1|$, the resulting expression is

$$\Omega(q) = (q^2/\rho e^2 s^2)\operatorname{Re}\left[\sigma_1\sigma_2(C_1 \pm C_2)^2/\sigma_1 + \sigma_2\right]. \tag{26}$$

Assuming that the impurity band[28] could be treated as a normal conducting band of electrons, the positive sign is appropriate for Eq. (26) and the effect of going from $q \gg q_{TF}$ to $q \ll q_{TF}$ would amount to a step down (or up) in the linearly varying scattering frequency by a ratio of approximately σ_2 to σ_1. This is in contrast to the extremely rapid ($> q^3$) fall in $\Omega(q)$ below q_{TF} in the case of a single band.

Should we instead consider the case of the light-hole band, the negative sign applies and, owing to

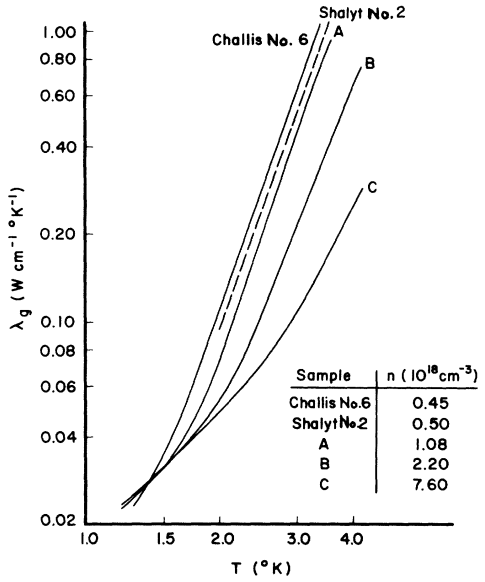

FIG. 4. Lattice thermal conductivity λ_g of five samples of heavily doped p-type InSb vs T in a log-log plot. The data for the most heavily doped samples of Challis *et al.* (No. 6 of Ref. 2) and of Shalyt (No. 2 of Ref. 30) are shown with data for the three samples described in this work. The data for Challis's sample No. 6 was analyzed using the method outlined here with the result for the values of the parameters: $C = -1.25$ eV, $d = 16.5$ °K^{-4}sec^{-1}, $\Theta^* = 15.5$ °K, and $q^e_{TF} = 0.87 \times 10^6$ cm^{-1}. These values are in good agreement with the values for sample A, B, and C presented in Table II. The data of Shalyt No. 2 falls as expected between Challis's No. 6 and sample A.

the near equality of C_1 and C_2 in this case, the scattering frequency is negligible. Thus, the light-hole band does not appear to assist in explaining the added scattering.

No attempt was made to use Eqs. (25) and (26) to analyze the data under the impurity-band hypothesis due to the additional unknown parameters, but it may be seen that his process would work in the desired direction to compensate for the screening.

Some justification for the neglect of the scattering terms given in Eqs. (7) and (8) may be presented here. The scattering represented by both of these terms depends on resonance phenomena—the first a resonance with localized phonon modes due to the presence of impurities and the second a bound electron-phonon resonance associated with localized impurity states. For both types of resonance scattering the depth of the "dip" in the thermal conductivity as plotted versus temperature varies with the concentration of impurities while the location of the dip along the temperature axis does not change. This is opposed to the data presented here in which the depth of the dip remains approximately constant and the location of the minimum shifts to higher temperatures as the doping increases.

Further evidence favoring the neglect of resonance scattering are the recent results of Shalyt *et al.*,[29] who obtained the same conductivity for two n-type samples with the same carrier concentration but different acceptor-donor concentrations.

This indicates that the scattering due to localized phonon modes and to localized bound-electron states associated with the acceptor impurities are not influential factors in the existence of the conductivity minimum. This agrees with the conclusion of the present work that the conductivity minimum is due to scattering by free charge carriers.

For comparison, the data for the samples studied here along with the data for the most heavily doped samples by Challis and Shalyt are presented in Fig. 4.

V. CONCLUSIONS

It has been shown that the lattice thermal conductivity of degenerate p-type InSb at helium temperatures can be successfully accounted for with a phenomenological model in which a principal phonon-scattering mechanism is due to charge carriers. The other mechanisms included in this model are Rayleigh scattering due to impurities and isotopes and boundary scattering.

Partial plasma screening in the charge-carrier–phonon interaction seems also to explain some conductivity features.

This model with emphasis on carrier-phonon scattering has been chosen, with some justification, in preference to a model in which phonon scattering by ionized impurities is a dominant mechanism.

ACKNOWLEDGMENTS

The authors are indebted to Professor John T. Marshall for reading the manuscript and for several helpful suggestions. The financial assistance received from the Dr. Charles E. Coates Memorial Fund of the Louisiana State University Foundation, donated by George H. Coates for the preparation of this manuscript is gratefully acknowledged.

---

*Work was performed under the auspices of the U. S. AEC and is AEC Report No. ORO-3087-45 (unpublished).

[1]L. J. Challis, J. D. Cheeke, and D. J. Williams, in *Proceedings of the Ninth International Conference on Low Temperature Physics* (Plenum, New York, 1965), p. 1145.

[2]R. S. Blewer, N. H. Zebouni, and C. G. Grenier, Phys. Rev. 174, 700 (1968).

[3]M. H. Cohen, M. J. Harrison, and W. A. Harrison, Phys. Rev. 117, 937 (1960).

[4]M. J. Harrison, Phys. Rev. 119, 1260 (1960).

[5]H. N. Spector, Phys. Rev. 127, 1084 (1962).

[6]H. N. Spector, in *Solid State Physics*, Vol. 19, edited by F. Seitz and D. Turnbull (Academic, New York, 1966), p. 291.

[7]A. B. Pippard, Phil. Mag. 46, 1104 (1955); Proc. Roy. Soc. (London) A257, 165 (1960).

[8]Nobuo Mikoshiba, J. Phys. Soc. Japan 12, 1691 (1959); 15, 982 (1960); 16, 895 (1961).

[9]E. I. Blount, Phys. Rev. 114, 418 (1959).

[10]S. G. Eckstein, Phys. Rev. 131, 1087 (1963).

[11]M. G. Holland, Phys. Rev. 134, A471 (1964).

[12]J. A. Carruthers, T. H. Geballe, H. M. Rosenberg, and J. M. Ziman, Proc. Roy. Soc. (London) A238, 502 (1957).

[13]J. A. Carruthers, J. F. Cochran, and K. Mendelssohn, Cryogenics 2, 160 (1962).

[14]Cominco American Inc., Spokane Industrial Park, Spokane, Washington 99216.

[15]There is a consensus [Gaston Fischer, Helv. Phys. Acta 33, 463 (1960); H. J. Hrostowski, F. J. Morin, T. H. Geballe, and G. H. Wheatley, Phys. Rev. 100, 1672 (1955); H. P. R. Frederikse and W. R. Hosler, *ibid.* 108, 1146 (1957); C. H. Champness, Phys. Rev. Letters 1, 439 (1958)] of results which indicates that the values of n listed in Table I and used in calculations throughout this work should be increased by a factor of between 1.3 and 1.5. The quantities which would be effected by an increase in the carrier density are τ_e, l_e, k_F, c, d, and Θ*.

[16]Joseph Callaway, Phys. Rev. 113, 1046 (1959); 122, 787 (1961).

[17]R. F. Potter, Phys. Rev. 103, 47 (1956).

[18]H. B. G. Casimir, Physica 5, 495 (1938).

[19]P. G. Klemens, in *Solid State Physics*, Vol. 7, edited by F. Seitz and D. Turnbull (Academic, New York, 1958), p. 1.

[20]R. O. Pohl, Phys. Rev. Letters 8, 481 (1962).

[21]R. W. Keyes, Phys. Rev. 122, 1171 (1961).

[22]J. M. Ziman, Phil. Mag. 1, 191 (1956); *Electrons and Phonons* (Oxford U. P., London, 1960), pp. 329–330.

[23]E. H. Sondheimer, Proc. Phys. Soc. (London) A65, 561 (1952).

[24]Usually $\alpha = 1$ unless the recombination strongly depends on compressive deformation and the recombination time is short. The dependence of α on ω has not been developed in view of the uncertainties involved. Even though computations were made with values of α other than unity, the final analysis uses $\alpha = 1$ only.

[25]*Materials Used in Semiconductor Devices*, edited by C. A. Hogarth (Interscience, New York, 1965), pp. 135, 150.

[26]E. F. Steigmeir and B. Abeles, in *Proceedings of the Seventh International Conference on the Physics of Semiconductors* (Academic, New York, 1965), p. 701.

[27]For acceptor doping levels such that indium antimonide is degenerate at liquid-helium temperatures, it is expected that an "impurity band" is formed in which there could be a conduction mechanism at least as efficient as the hopping of electrons from one impurity site to another. The carriers in this band, which for acceptor impurity concentrations above 2×10^{17} cm^{-3} overlap the valence band [R. F. Broom and A. C. Rose-Innes, Proc. Phys. Soc. (London) B69, 1269 (1956)], have a small conductivity which should increase with increased doping.

[28]The condition $\sigma_2^0 < \sigma_1^0$ does not induce the same relationship between the σ_i. For the impurity band, the conditions $ql_2 < ql_1$ and $\omega\tau_2 < \omega\tau_1$ yield $\sigma_2' > \sigma_1'$, and this may give values of σ_1 and σ_2 of comparable magnitude. It is expected that in the present case $\sigma_2 < \sigma_1$, where index 1 refers to the heavy-hole band and index 2 refers to the impurity band.

[29]S. S. Shalyt, P. V. Tamarin, and V. S. Ivleva, Phys. Letters 32A, 29 (1970).

PHYSICAL REVIEW B VOLUME 4, NUMBER 4 15 AUGUST 1971

Dielectric Screening and the Mott Transition in Many-Valley Semiconductors

J. B. Krieger* and M. Nightingale†
Department of Physics, Polytechnic Institute of Brooklyn, Brooklyn, New York 11201
(Received 8 March 1971)

We show that the donor density N_c required for the Mott transition to occur in a many-valley semiconductor is given by $a_0(N_c)^{1/3} = 0.25C(\nu)$, where a_0 is the radius of the first Bohr orbit in the material, ν is the number of equivalent conduction-band valleys occupied by electrons, and $C(\nu) = \nu^{-2/3}$ in the Thomas-Fermi (TF) approximation. This result is identical to Mott's for $\nu = 1$ and is in good agreement with experiment for that case, but predicts an N_c which is smaller than the experimental results for Ge ($\nu = 4$) and Si ($\nu = 6$). This discrepancy is attributed to the fact that the TF approximation does not include the result, predicted by the dielectric-screening theory, that only those Fourier components of the potential for which $q \lesssim 2k_F$ are effectively screened by the conduction electrons. This is of increased significance in the many-valley case due to the decrease of k_F for a given N. We have calculated the condition for zero activation energy assuming dielectric screening and find $C(1) = 1.14$, $C(2) = 0.96$, and $C(4) = C(6) = 0.92$ in good agreement with the available experimental results. We also note that it may be possible to observe a metal-to-insulator transition when stress is applied to a degenerately doped Ge crystal.

I. INTRODUCTION AND CONCLUSIONS

It is well known that as the density of donors in a semiconductor increases, the activation energy decreases owing to the electron-electron interaction and that for sufficiently high donor concentrations the activation energy will vanish resulting in metallic conduction.[1] It was Mott who first pointed out that this insulator-to-metal transition might be abrupt with a definite critical density which experimentally appears to be slightly smeared out because of the variation in the local density of donors about the average density.[2]

In order to get an estimate of the critical density N_c at which the transition would occur, Mott assumed Thomas-Fermi screening of the donor atoms by the electrons and found the condition for zero activation energy, i.e., when the binding energy of the electron to the donor is zero. The result was

$$a_0 N_c^{1/3} \cong 0.25, \tag{1}$$

where a_0 is the first Bohr orbit in the material. Mott[3] and Mott and Twose[4] found that there was good agreement between theory and experiment for heavily doped Ge and Si, the constant on the right-hand side of Eq. (1) being approximately 0.2. More recently Alexander and Holcomb[5] have made a detailed analysis of the transport data on Si : P,[6] Ge : Sb,[7–9] Ge : P,[8] Ge : As[8] and found that the average value of the constant in Eq. (1) is 0.22. In each case, the value of the effective mass appearing in a_0 was taken as the one that gave the experimentally observed binding energy of an electron bound to a donor in the light-doping range for each particular dopant.